Tetramethylpyrazine Derivative T-006 Ameliorates the Amyloid-β Plagues of Transgenic Alzhermer's Mice by Modulation of TLR4-mediated MyD88/NF-κB Signaling

Haiyun Chen
Guangdong Pharmaceutical University
Xiao Chang
Guangdong Pharmaceutical University
Jiemei Zhou
Guangdong Pharmaceutical University
Guiliang Zhang
Jinan University
Jiehong Cheng
Jinan University
Zaijun Zhang
Jinan University
Zheng Liu (Liuzheng8709@gmail.com)
Foshan University
Chunyan Yan
Guangdong Pharmaceutical University

Research

Keywords: Microglial activation, neuroinflammation, Alzheimer's disease, tetramethylpyrazine derivative, signaling pathways

Posted Date: November 22nd, 2021

DOI: https://doi.org/10.21203/rs.3.rs-1043837/v1

Abstract

Background

Microglial activation mediated neuroinflammation was considered as a vital trigger factor in the pathogenesis of Alzheimer's disease (AD). T-006, a new tetramethylpyrazine derivative, has been recently found to alleviate cognitive deficits via inhibition of Tau expression and phosphorylation in AD transgenic mouse models. Here, we hypothesized that T-006 may ameliorate AD-like pathology by suppressing the neuroinflammation.

Methods

APP/PS1 transgenic AD mouse model was used here to evaluate the anti-inflammatory effect of T-006 and its underlying mechanisms, as well as its potential protective effects against lipopolysaccharide (LPS)-activated microglial-induced neurotoxicity.

Results

Our results indicated that T-006 significantly decreased the levels of total amyloid β peptide (Aβ) and glial fibrillary acidic protein (GFAP) as well as the ionized calcium binding adaptor molecule-1 (Ibα-1) expression in the APP/PS1 mice. Moreover, T-006 dramatically suppressed abnormal elevation of inflammatory mediators and reduced the levels of Toll-like receptor 4 (TLR4), myeloid differential protein-88 (MyD88) and NF-κB signaling related proteins in lipopolysaccharide (LPS)-induced BV2 microglial cells. We also found that TAK242, a TLR4 inhibitor could abolish the down-regulation of T-006 on LPS-induced proinflammatory mediators and reversed the downstream proteins expression containing MyD88 and NF-κB signaling. Importantly, T-006 prevented against neuroinflammation induced neurotoxicity by mitigating reactive oxygen species (ROS) overproduction and mitochondrial membrane potential (MMP) dissipation.

Conclusions

T-006 exerts neuroprotective effect in treating AD by suppressing the neuroinflammation through modulation of TLR4-mediated MyD88/NF-κB signaling pathways.

1. Introduction

Alzheimer's disease (AD), a complex degenerative disease of central nervous system (CNS), is characterized by the decline of memory and cognitive ability. The extracellular deposits of amyloid β peptide (Aβ) in senile plaques (SP) and the formation of intracellular neurofibrillary tangles (NFTs) caused by the hyperphosphorylation of Tau protein, are consisted of the most two important neuropathological features of AD, which contributed to the synapse loss and neurons death, and subsequently memory impairment [1]. Over 200 reagents targeting Aβ or Tao protein were researched in recent decades aimed to reverse or stop the degeneration progress of AD, but unfortunately, none is

currently clinical available [2]. The underlying failure is that targeting the pathological features rather than the pathogenic factors seems an endless parade of the pharmaceutical anti-AD development [3]. Therefore, elucidating the precise mechanisms underlying the AD and seeking efficient agents with disease-modifying potential becomes the focus of current research.

Although the etiology of AD is not fully understood, increasing evidences confirmed that microglial activation mediated neuroinflammation was one of the vital trigger factors of AD [4, 5]. Neuroinflammation is an important neuropathological process, which is triggered by microglia and astrocytes activation and closely related to the brain injury and neurodegenerative diseases including AD and Parkinson's disease [6, 7]. Especially, microglia acted as the main immune-surveillance cells of CNS, of which over-activation increased pathological Aβ and Tau accumulation and synapse loss, and subsequently resulted in neuronal damage and death [8, 9]. Therefore, inhibition of microglial activation and reduction of inflammatory mediators production is considered as beneficial strategy in AD therapy [10, 11].

Tetramethylpyrazine (TMP) is the main active component of Chinese herb *Ligusticum* (Chuanxiong), which is widely used in clinical treatment of hypoxic-ischemic encephalopathy and cerebro-cardiovascular diseases due to its ability to penetrate blood brain barrier (BBB) to generate therapeutic effects [12, 13]. J147 is a multifunctional neuroprotectant with great potential to improve the degenerative process of AD, and its phase I clinical trial against AD was completed in 2020 (NCT03838185). In order to make full use of the advantages of TMP and improve its activity, we have synthesized a new TMP derivative named T-006 by replacing the methoxybenzene ring of J147 with TMP. In previous studies, we found that T-006 alleviated cognitive deficits via inhibition of Tau and APP expression in AD transgenic mice models [14]. However, the specific mechanism underlying the anti-AD effect of T-006 is unclear and whether this effect is regulated by the anti-neuroinflammation ability is still unknown. The present study thus aimed to investigate the anti-inflammatory effect of T-006 prophylactic treatment on a transgenic AD model and its underlying mechanisms, as well as its potential protective effects against lipopolysaccharide (LPS)-activated microglial-induced neurotoxicity.

2. Materials And Methods

2.1. Chemicals and reagents

All media and supplements used for cell cultures were purchased from Gibco (Carlsbad, CA, USA), unless otherwise marked. LPS, Poly-L-Lysine (PLL), and 3-(4, 5-dimethyl-2-thiazyl)-2, 5-diphenyl-2H-tetrazolium bromide (MTT) were obtained from Sigma-Aldrich (St. Louis, MO, USA). JC-1 kit, 2, 7′dichlorofuorescin diacetate ($DCFH_2$-DA) and Hoechst 33342 were obtained from Beyotime (Beyotime, China). RIPA lysis buffer, phenylmethanesulfonyl fluoride (PMSF), and halt phosphatase inhibitor cocktail were purchased from Pierce Biotechnology (Rockford, IL). TAK242 was obtained from APExBIO (Huston, USA). Antibodies against Aβ, glial fibrillary acidic protein (GFAP), ionized calcium binding adaptor molecule-1 (Ibα-1), Toll-like receptor 4 (TLR4), myeloid differential protein-88 (MyD88), NF-κB p65, phospho-p65, inducible nitric

oxide synthase (iNOS) and cyclooxyganese-2 (COX2) were obtained from Cell Signaling Technology (Beverly, MA, USA). Antibodies against β-actin and proliferating cell nuclear antigen (PCNA) were obtained from Proteintech (Wuhan, China). All other reagents were from Sigma-Aldrich (St. Louis, MO) except where stated otherwise.

2.2. Animals and treatment

The APP/PS1 mice were purchased from Jackson Laboratory and housed in a 12 h light/dark cycle under conditions of controlling humidity at 50 ± 10% and temperature at 22 ± 2°C. All experiments were performed in accordance with the guidelines from the Laboratory Animal Care and Use Ethics Committee of the Shenzhen Center for Disease Control and Prevention. Wide type (WT) and APP/PS1 mice were randomly divided into following groups (n=8-10/group): WT (Sham group), APP/PS1 (vehicle group), APP/PS1 + T-006 (3 mg/kg). Mice in T-006 group were administrated intragastrically once a day, while the sham group mice and vehicle group mice received equal volume of saline.

2.3. BV2 cells cultures

BV2 cells obtained from Cell Resource Center of the Institute of Basic Medical Sciences at the Chinese Academy of Medical Sciences (Beijing, China) were grown in Dulbecco's Modified Eagle's Medium with Nutrient Mixture F-12 (DMEM/F-12), supplemented with 10% (v/v) fetal bovine serum (FBS), and 1% (v/v) penicillin/streptomycin mixture. Cells were seeded in 96-well plates (100 μL/well) at a concentration of 5×10^4 cells/mL. Cultures were maintained in an incubator at 37°C with humidified atmosphere containing 5% CO_2. Experiments were carried out 24 h after the cells were seeded.

2.4. PC12 cells cultures

PC12 cells obtained from Jinan University (Guangzhou, China) were maintained in DMEM/F-12, supplemented with 12.5% FBS and 2.5% horse serum, as well as 1% penicillin/streptomycin mixture. Cells were seeded in 96-well plates (100 μL/well) at a concentration of 1.2×10^5 cells/mL in a humidified environment of 5% CO_2 at 37°C. Experiments were carried out 24 h after the cells were seeded.

2.5. MTT assay

The tetrazolium salt 3-(4,5-dimethylthiazol-2-yl)-2,5-diphenyltetrazolium bromide dye (MTT) assay was used to evaluate neurotoxicity. The assay was performed as our described previously with minor modifications (Chen et al., 2015). Briefly, BV2 cells were pre-treated with/without T-006 (1, 3, 10 μM) and minocycline (MINO, 5 μM) for 2 h before exposure to LPS (1 μg/mL) for 24 h. Control group denotes the cells were cultured in normal-medium. For neuroprotective experiment, the culture medium collected from BV2 cells exposed to 1 μg/mL LPS for 24 h was used as the activated microglia-conditioned medium (L-CM), which is performed as previous publication [15]. Then PC12 cells that treated with T-006 (1, 3, 10 μM) or MINO (5 μM), were cultured in L-CM for another 24 h. MTT (10 μL, 5 mg/mL) was added into the culture medium and cells were cultured at 37 ^oC for 4 h. After dissolving the formazan by replacing the medium with 100 μL of DMSO, the absorbance of the samples at 570 nm were read and recorded by a microplate reader (Molecular Service, USA).

2.6. Nitric oxide (NO) detection

The accumulation of NO in cell culture supernatant was detected by Griess reaction [16]. Concretely, BV2 microglial cells (3×10^4 cells/well) were seeded into 96-well plates and treated with T-006 (1, 3, 10 μM) for 2 h. After incubated with LPS (1 μg/mL) for 24 h, 50 μL of culture supernatant was mixed with equal volume of Griess reagent for 10 min at room temperature in the dark. Then, the absorbance was determined at 540 nm using a microplate reader.

2.7. Intracellular reactive oxygen species (ROS) detection

PC12 cells were seeded on 96-well plates and incubated with T-006 (1, 3, 10 μM, dissolved in L-CM) or MINO (5 μM, dissolved in L-CM) for 24 h. Control denotes normal-medium cultured cells. The total intracellular ROS were detected by incubating with $DCFH_2$-DA (10 μM) for 30 min. The uorescence intensity was measured on a microplate reader at 495 nm excitation and 530 nm emission, respectively. After the measurement of fluorescence intensities, cell viability was measured by MTT assay. The extent of inhibition on ROS and RNS production was reflected by the mean fluorescence intensities. The mean uorescence intensities were calculated by the formula: mean uorescence intensities (%) = detected uorescence intensities/cell viability × 100.

2.8. ATP measurement

PC12 cells were seeded on 96-well plates and incubated with T-006 (1, 3, 10 μM, dissolved in L-CM) or MINO (5 μM, dissolved in L-CM) for 24 h. Control denotes normal-medium cultured cells. The intracellular ATP was measured using an ATP Assay kit (Beyotime, China), of which the values in each treated group were calculated as a percentage of the control.

2.9. Mitochondrial membrane potential (MMP) measurement

PC12 cells were seeded on 96-well plates and incubated with T-006 (1, 3, 10 μM, dissolved in L-CM) or MINO (5 μM, dissolved in L-CM) for 24 h. Control denotes normal-medium cultured cells. After three times washed with ice-cold PBS, neurons were incubated with JC-1 (2 μM) for 10 min. The fluorescence intensity was measured on a microplate reader at 490 nm/530 nm dual excitation and 525 nm/590 nm dual emissions. MMP was reflected by the ratio of fluorescence intensity at 590 nm/530 nm.

2.10. Cytokine enzyme-linked immunosorbent (ELISA) assays

BV2 cells were cultured in 96-well plate at a density of 5×10^4 cells/mL for 24 h. After treatment with 50 nM TAK242 (a TLR4 receptor inhibitor) for 30 min, cells were treated with T-006 (1, 3, 10 μM) or MINO (5 μM) for 2 h and then exposed to LPS (1 μg/mL) for 24 h. Control denotes normal-medium cultured cells. The concentrations of TNF-α and IL-6 in the culture supernatant were determined by ELISA assay kit

according to the manufacturer's instructions (Elabscience Biotechnology, Wuhan, China). The absorbance of the sample at 450 nm was measured by a microplate reader.

2.11. Real-time reverse-transcription polymerase chain reaction (RT-PCR)

Total RNA was extracted from the cultured cells using Axygen total RNA miniprep kit (Corning, USA) and cDNA was obtained from the RNA using Hifair-II 1st Strand cDNA Synthesis SuperMix (Yeasen Biotechnology, China), according to the manufacturer's instructions. Real-time PCR (RT-PCR) program was executed as previous publication (Woo et al., 2014). In brief, Hieff® qPCR SYBR Green Master Mix and a Roche light cycler 96 sequence detection systems (Roche) were involved in the complement of RT-PCR. The primer sequences used were as follows: COX2: TGCACTATGGTTACAAAAGCTGG (forward) and TCAGGAAGCTCCTTATTTCCCTT (reverse); TNF-α: CTGAACTTCGGGGTGATCGG (forward) and GGCTTGTCACTCGAATTTTGAGA (reverse); IL-6: TCTATACCACTTCACAAGTCGGA (forward) and GAATTGCCATTGCACAACTCTTT (reverse); IL-1β: CTGTGACTCATGGGATGATGATG (forward) and CGGAGCCTGTAGTGCAGTTG (reverse); GAPDH: CATGTTCCAGTATGACTCCACTC (forward) and GGCCTCACCCCATTTGATGT (reverse). All data were expressed relative to GAPDH expression and quantified by Roche internal software.

2.12. Immunofluorescence staining

BV2 cells were seeded on sterile coverslips in the 24-well plate at the density of 5×10^4 cells/mL for 24 h. After pretreated with T-006 (3, 10 μM) for 2 h, LPS (1 μg/mL) was added and incubated for 24 h, 12 h and 30 min, respectively. Control denotes normal-medium cultured cells. Cells were washed with ice-cold PBS and fixed with 4% PFA in PBS for 30 min at room temperature. Subsequently, cells were blocked using 5% BSA blocking buffer for 1 h at room temperature before incubated with antibodies against TLR4 and NF-κB p65 overnight at 4°C. The cells were then washed with ice-cold PBS and incubated with secondary Alexa Fluor 488 and 594 labeled antibodies supplemented with DAPI (5 μM) for 2 h at room temperature in the dark. The coverslips were mounted and photos were taken under a fluorescence microscope at 400× magnification (Vert. A1, Zeiss, Germany).

2.13. Immunohistochemical staining

Mice were anesthetized with pentobarbital sodium (50 mg/kg; i.v.) and sacrificed after the behavioral experiment, and then fixed with 4% paraformaldehyde. Subsequently, brain tissue was embedded in paraffin, and cut to make 5-μm thick serial coronal sections for Aβ, GFAP and Ibα-1 immunohistochemical staining, as our previous described [17]. The number of Aβ plaques and the GFAP- and Iba1-positive cells were identified using a fluorescence microscope (Olympus, Japan), and then blindly counted via ImageJ (NIH, Bethesda, MD, USA).

2.14. Western blot assay

Western blot assay was performed as previously described [18]. Concretely, Brain tissues or cells were harvested using RIPA lysis buffer containing a cocktail of protease and phosphatase inhibitors. Subsequently, the total cytosol and nuclear proteins were isolated and their concentrations were determined by the BCA assay (Pierce, Rockford, IL, USA). The proteins (20-30 μg) were separated on a 10% SDS–polyacrylamide gel and then transferred to the polyvinyldifluoride membrane. After blocking with a 5% BSA blocking buffer, the polyvinyldifluoride membranes were co-incubated using primary antibodies overnight at 4 ^{O}C respectively against TLR4, MyD88, NF-κB p65, phospho-p65, iNOS, COX2, β-actin and PCNA. Subsequently, the membranes were then washed with TBST and incubated with secondary antibodies at room temperature for 2 h. The signals were obtained using an ECL Plus kit using a detecting system (ProteinSimple, USA). Finally, the quantitative analysis was provided by ImageJ (NIH, Bethesda, MD, USA).

2.15. Data analysis

All data presented as means ± SEM were carried out at least three times independent experiments. Analysis of one-way ANOVA with Dunnett's test was used for multiple experimental statistical comparisons, with $P < 0.05$ being considered as statistical significance.

3. Results

3.1. T-006 alleviated the Aβ accumulation in the hippocampus of the APP/PS1 mice

As reported, Tau tangles and Aβ plaques are two important hallmarks of AD. Previously, we found that T-006 improved cognitive ability after a long-term administration in AD transgenic mice of both APP/PS1-2xTg and APP/PS1/Tau-3xTg. Importantly, T-006 mitigated cognitive decline in 3xTg mice primarily via reducing the p-Tau and total Tau levels [14]. Thus, we wondered whether T-006 alleviated Aβ expression. Here, the Aβ expression levels in the brain of APP/PS1 mice, and quantify the Aβ plaques in the cortex and hippocampus were assessed. As illustrated in Fig. 1A-C, the Aβ deposition in APP/PS1 mice brain was obviously overexpressed both in the cortex and hippocampus compared to the WT mice. However, the T-006 treatment significant reduced Aβ deposition in the hippocampus, but not in the cortex. To further confirm which Aβ fractions were affected by T-006, Elisa analysis was used to test the soluble and insoluble forms of Aβ extracted from the hippocampus. The results showed that there was no significant difference in the soluble fractions of both Aβ1-42 and Aβ1-40 with or without T-006 treatment in APP/AS1 mice, while the insoluble fraction levels of both Aβ1-42 and Aβ1-40 were strikingly decreased in T-006 treatment group (Fig. 1D-G).

3.2. T-006 suppressed neuroinflammation in the APP/PS1 mice

Chronic neuroinflammation characterized with the abnormal activation of microglia and astrocytes has been observed in AD patients and AD animal models, respectively [19]. We next explored whether T-006 can attenuate neuroinflammation in AD mice. The immunostained assay of brain sections with antibodies against the GFAP and Ibα-1, which respectively represented a specific marker of astrocyte and microglia, was performed. As shown in the Fig. 2A-C, compared with the WT mice, the activation of astrocytes and microglial were dramatically elevated in the hippocampus of the APP/PS1 mice. However, microglial activation, but not astrocytes activation, was significantly repressed by T-006 treatment in APP/PS1 mice. Western blot analysis also demonstrated that T-006 obviously down-regulated the Ibα-1 proteins expression of hippocampus in APP/PS1 mice (Fig. 2D **and E**).

3.3. T-006 diminished LPS-stimulated pro-inflammatory cytokine responses in BV2 microglial cells

Firstly, the cell cytotoxicity of T-006 on BV-2 cells was tested and results suggested that T-006 (1, 3 or 10 μM) had no cytotoxic effect on BV-2 cells for 24 h (Fig. 3A). Then the NO production of cells was detected. The result in Fig. 3B showed that LPS at the concentration of 1 μg/mL robustly stimulated the NO overproduction, while T-006 or MINO treatment significantly reversed the LPS-induced NO overproduction in BV2 cells. Importantly, the effect of T-006 at 10 μM was stronger than that of MINO. We next evaluated the effects of T-006 on the expression of IL-1β and TNF-α in LPS-stimulated BV-2 cells. The Elisa results revealed that T-006 significantly reversed the up-regulation of IL-1β and TNF-α proteins expression induced by LPS (Fig. 3C **and D**). Additionally, as illustrated in Fig. 1E–H, the mRNA levels of pro-inflammatory cytokines and mediators of COX2, TNF-α, IL-1β and IL-6 were markedly increased in LPS treated groups. Pretreatment with T-006 (1-10 μM) concentration dependently prevented LPS-induced increases in pro-inflammatory mediators, while T-006 treatment alone did not affect the levels of these proinflammatory cytokines compare with the control. Subsequently, we detected the protein expression of iNOS and COX2 through Western blot, and results revealed that LPS treated alone significantly up-regulated the iNOS and COX2 proteins expression, which was also obviously attenuated by T-006 treatment (1-10 μM) in a concentration dependent manner (Fig. 3I–L).

3.4. T-006 suppressed the expression of TLR4 and its down-regulator MyD88 in LPS-induced BV2 microglial cells

TLR4 was considered as an important receptor of LPS, which could interact with a specific adaptor molecular MyD88 and regulate inflammatory responses via activating the downstream signaling pathway including NF-κB [20]. Thus, whether the T-006 could modulate the TLR4 and its adaptor molecular MyD88 levels were investigated. As shown in Fig. 4A-C, pretreated with T-006 statistically inhibited the sharp increasement of TLR4 and MyD88 expression levels triggered by 1 μg/mL of LPS in BV2 cells. Consecutively, the immunofluorescence staining with TLR4-specific antibody also demonstrated that T-006 at the concentrations of 3 and 10 μM down-regulated LPS-induced TLR4 overexpression in BV2 microglial cells (Fig. 4D).

3.5. T-006 inhibited the activation of NF-κB pathway in LPS-activated BV-2 microglial cells

Increasing evidence indicated that NF-κB signaling pathway played a vital role in regulating microglial-mediated inflammatory processes [21–23], and previous work reported that inhibition of NF-κB-driven gene transcriptional activity effected potent anti-inflammation against LPS-stimulated microglial cells activation [24]. Therefore, the effects of T-006 on NF-κB signaling pathway were also examined here. As shown in Fig. 5A **and B**, LPS markedly induced the expression of phosphorylation of NF-κB p65. In contrast, T-006 treatment concentration-dependently inhibited the phospho-NF-κB p65, which indicated that T-006 inhibited NF-κB signaling activation [25]. The findings were also reinforced by immunofluorescence staining of the intracellular NF-κB p65 subunit. T-006 abrogated the LPS-evoked nuclear translocation of NF-κB p65 (Fig. 5C). These results suggested that T-006 alleviated LPS-induced neuroinflammation by inhibiting the activation of NF-κB signaling pathway.

3.6. T-006 diminished LPS-induced proinflammatory cytokines levels through suppression of TLR4-mediated MyD88/NF-κB pathway

To further confirm the inhibition of TLR4/MyD88 signaling pathway was associated with anti-inflammatory effect of T-006 against the LPS-induced microglial activation, the specific TLR4 inhibitor TAK242 was pretreated before BV2 cells exposure to T-006. The proteins expression of iNOS and COX2 were measured through Western blot. Expectedly, both T-006 (3 μM) and TAK242 (100 nM) administration robustly reversed the proteins expression increase of iNOS and COX2 induced by LPS, while no significance was observed between co-treatment with TAK242 and T-006 and TAK242 treated alone. Additionally, we found that T-006 treatment alone had no effect on these two proteins expression, which was consistent with the above finding that T-006 did not affect the levels of these proinflammatory cytokines under basal conditions (Fig. 6A-C). Since MyD88 acted as an important downstream targeting molecular adaptor of TLR4 [26], the effect of TAK242 on T-006's modulation of MyD88 expression was further investigated. As shown in Fig. 6D **and E**, T-006 significantly decreased the up-regulation of MyD88 protein levels in LPS-evoked BV2 microglial cells. However, treatment with combination of TAK242 (100 nM) and T-006 (3 μM) did not showed a stronger inhibitory effects compared to TAK242 or T-006. TLR4 depletion was reported to contribute to the inhibition of NF-κB signaling pathway [20]. Whether T-006's inactivation of the NF-κB signaling pathway was affected by TLR4 inhibitor TAK242 or not is unclear. As shown in Fig. 6F and **G**, T-006 considerably mitigated the LPS-induced phospho-NF-κB p65, whereas the addition of TAK242 did not affect this reversion effect of T-006. The immunofluorescent assay further confirmed the results that TLR4 inhibitor TAK242 did not affect the effect of T-006 on NF-κB signaling pathway. These data suggested that T-006 suppressed the pro-inflammatory responses in LPS-activated BV2 microglial cells via TLR4-mediated MyD88/NF-κB signaling pathway.

3.7. T-006 protected against LPS-activated BV2 microglia-mediated neurotoxicity in PC12 cells

Since T-006 presented suppressive effects on neuroinflammation in LPS-activated microglia, the effects of T-006 against neuroinflammation-mediated neurotoxicity in PC12 cells under L-CM induction was also evaluated. As expected in the Fig. 7A, L-CM caused an obvious reduction (approximately 48.6%) in the viability of PC12 cells. Conversely, T-006 (1, 3, 10 μM) significantly attenuated the L-CM-caused cytotoxicity in a concentration-dependent manner. The cell viability of T-006 at 10 μM is higher than that of the positive control MINO (5 μM). In line with our previous finding [15], the vehicle-treated medium (vehicle group) did not affect the cell viability. As reported, the intracellular ROS overproduction is tightly involved in a cascade of harmful events, which ultimately induce neuronal damage and death [25]. Thus, intracellular ROS production was tested here and the result suggested that pretreatments with T-006 from 1 to 10 μM and MINO (5 μM) significantly reduced the ROS accumulation compared to the L-CM stimulation (Fig. 7B). To evaluate whether the neuroprotective effects of T-006 was related to maintenance of mitochondrial function, which acted as an important participants in inflammation-mediated injury [27]. We tested the ATP release and the mitochondrial membrane potential (MMP) collapse under L-CM stimulation. As presented in the Fig. 7C, pretreatment with T-006 concentration-dependently and noticeably attenuated ATP decrease in L-CM co-treated PC12 cells. Additionally, the L-CM-induced MMP collapse was considerably reversed by T-006 treatment, indicating that the neuroprotective effect of T-006 was dependent on stabilizing MMP to preserve mitochondrial function (Fig. 7D **and E**).

4. Discussion

Neuroinflammation, a self-defense reaction initiated by the central nervous system (CNS) in the brain injury, has been suggested as a causal factor in the pathogenesis and progression of many neurodegenerative diseases [7]. Although many anti-AD drugs targeting amyloid and Tau hypothesis failed to reach the clinical endpoints in past decades, a window was opened that neuroinflammation might be a new key pathogenic factor of AD, among which microglial-activated neuroinflammatiory responses by releasing a variety of proinflammatory cytokines could result in neurological injury [28]. Therefore, suppressing microglia-evoked neuroinflammation and reducing cellular injury may play an important role in AD therapy. In the current study, we showed that T-006 significantly decreased the Aβ accumulation by inhibiting neuroinflammation, and the anti-neuroinflammation effect of T-006 was tightly involved in the suppression of TLR4-meidated MyD88/NF-κB signaling. Importantly, T-006 provided neuroprotection against neuroinflammation-induced neuronal damage via attenuating ROS overproduction and subsequent mitochondrial dysfunction.

Although the etiology of AD is unclear, the brain Aβ pathology of SP has still be considered as the gold standard for AD diagnose since the decreased Aβ clearance is a common prelude to late-onset AD [29]. Here, we found that T-006 administration significantly reduced the deposition of Aβ in the hippocampus

of APP/PS1 mice (Fig. 1). In addition, our previous results suggested that T-006 could considerably down-regulated the expression levels of amyloid precursor protein (APP) and β-secretase (BACE-1) [14], which are key contributors of Aβ production [30]. Nevertheless, the failure of reducing the Aβ levels has achieved a consensus that only targeting the pathological products is far from enough for the strategy of anti-AD drugs development and there is an urgent need to understand the non-misfolded proteins pathogenesis in AD. As expected, inflammatory responses is closely linked with the activation of glia mainly including astrocytes and microglia in AD models, which are believed to initiate or aggravate the neurodegenerative processes by inducing Aβ oligomerization and tau hyperphosphorylation [1, 31]. In the current study, we found that both the activation of astrocytes and microglia were significant augmented in the hippocampus of APP/PS1 mice, while T-006 obviously reversed this over-activation of microglia, but there is no significant difference in the activation of astrocytes compared with the vehicle group (Fig. 2A-C). The Western blot assay further confirmed this inhibition of T-006 on the microglial activation by down-regulating the Ibα-1 expression level (Fig. 2D **and E**). These results suggested that T-006 could attenuate the Aβ deposition via the inhibition of microglial activation and its underlying precise mechanism also needs deeper investigation.

Microglia are the first responder to Aβ accumulation and its activation can initiate an inflammatory response by producing a large number of inflammatory molecules including TNF-α, IL-6, IL-1β, iNOS and COX2, which result in synaptic degeneration, neuronal cell death, and cognitive dysfunction [32]. Thus, the LPS was used here as stimulator of microglial activation to evaluate the anti-neuroinflammation activity of T-006. As shown in Fig. 3, LPS can increase TNF-α, IL-6 IL-1β, iNOS and COX2 expression levels. Not surprisingly, T-006 significantly and concentration-dependently reduced these proinflammatory molecules levels in LPS-induced BV2 microglia, implicating that T-006 attenuate aberrant microglial activation and subsequently over-activated microglia-induced inflammatory response. Accumulating evidence has shown that recognition of LPS by TLR4 plays a pivotal role in the neuroinflammation of AD, which can cause an overproduction of pro-inflammatory cytokines in response to neuronal dysfunction via activating MyD88/NF-κB downstream signaling [17, 33]. Thus, inhibition of TLR4 to block the occurrence of these pro-inflammatory cytokines, exhibits potential therapeutic effects for the treatment of AD [34]. Interestingly, in the current study, treatment with T-006 statistically inhibited the increased effects triggered by LPS on TLR4 and MyD88 expression levels (Fig. 4A-C). The immunofluorescence assay further confirmed that the down-regulation effect of T-006 on the TLR4 expression (Fig. 4D). Furthermore, we also evaluated the NF-κB expression affected by T-006. As illustrated in the Fig. 5, stimulation of LPS increased the phosphorylated NF-κB p65, resulting in a higher translocation of NF-κB p65 in nucleus, while T-006 effectively reversed this alteration. Furthermore, we assessed the action of TLR4 depletion in regulating T-006's anti-inflammatory effect using a TLR4 inhibitor TAK242. Consistent with the previous publication [35], TAK242 treatment significantly suppressed LPS-induced expression levels of iNOS and COX2, while co-treatment of T-006 with TAK242 did not abolish the down-regulation effect of TAK242 on these two pro-inflammatory factors (Fig. 6A-C). Subsequently, we examined whether TAK242 altered the effects of T-006 on TLR4 downstream signaling of MyD88/NF-κB. As expected, there is no significant difference between co-incubation of T-006 with TAK242 and TAK242 alone in the expression levels of

MyD88 and phosphorylated NF-κB p65 (Fig. 6D-H). Based on these results, we presumed that TLR4-mediated MyD88/NF-κB signaling pathway was tightly involved in the suppressive effect of T-006 on LPS-activated pro-inflammatory responses.

Several lines of studies have demonstrated that microglial activation caused overproduction of inflammatory molecules is a key contributor to neuronal injury [20, 25]. Therefore, the inhibition of neuroinflammatory processes by blocking these pro-inflammatory molecules might be able to confer neuroprotection. In this study, we used the L-CM co-incubation with PC12 cells to test the neuroprotective effects of T-006 against inflammation-caused cell damage. In line with our previous publication [15], L-CM resulted in a significant reduction in the cell viability, while this L-CM-induced cell reduction could be counteracted by T-006 (Fig. 7A). Subsequently, we measured the intracellular ROS and found that T-006 significantly prevented the intracellular ROS aggregation stimulated by activated microglia (Fig. 7B). As reported, intracellular ROS overproduction is related to mitochondrial permeability transition pore opening, which in turn causes mitochondrial depolarization and consequently neuronal injury [36]. In this study, we also found that T-006 could both mitigate ATP production and MMP dissipation (Fig. 7C-E). Altogether, these results imply that T-006 exerted potent neuroprotection against neuroinflammation-induced neuronal damage.

In summary, our current study elucidated that T-006 significantly decreased the levels of total Aβ and GFAP as well as the Ibα-1 expression in the APP/PS1 mice. Additionally, T-006 effectively inhibited LPS-induced neuroinflammation in BV2 microglial cells via inactivation of the TLR4-mediated MyD88/NF-κB signaling pathways, resulting in neuroprotection against neuroinflammation-induced neurotoxicity by reversing mitochondrial impairment. Our results suggested that T-006 exerts neuroprotective effect in treating AD by suppressing the neuroinflammation through modulation of TLR4-mediated MyD88/NF-κB signaling pathways.

Abbreviations

AD, Alzheimer's disease; CNS, central nervous system; Aβ, amyloid β peptide: SP, senile plaques; NFTs, neurofibrillary tangle; TMP, tetramethylpyrazine; PLL, Poly-L-Lysine; MTT, 3-(4, 5-dimethyl-2-thiazyl)-2,5-diphenyl-2H-tetrazolium bromide; LPS, lipopolysaccharide; PMSF, phenylmethanesulfonyl fluoride; $DCFH_2$-DA, 2, 7′dichlorofuorescin diacetate; Ibα-1, ionized calcium binding adaptor molecule-1; GFAP, glial fibrillary acidic protein; TLR4, Toll-like receptor 4; ROS, reactive oxygen species ; MMP, mitochondrial membrane potential; iNOS, induced nitric oxide synthase; COX2, cyclooxyganese-2; PCNA, proliferating cell nuclear antigen; MyD88, myeloid differential protein-88; DMEM/F-12, Dulbecco's modified Eagle's medium with nutrient mixture F-12; FBS, fetal bovine serum; L-CM, activated microglia-conditioned medium; MINO, minocycline; NO, Nitrix oxide.

Declarations

Ethics approval and consent to participate: All experiments were performed in accordance with the guidelines from the Laboratory Animal Care and Use Ethics Committee of the Shenzhen Center for Disease Control and Prevention. All efforts were made to ameliorate the suffering of animals. Deeply anesthetized mice were euthanized by perfusion followed by a physical method for tissue collection.

Consent for publication: Not applicable.

Availability of data and materials: All data generated or analyzed during this study are included in this published article.

Competing interests: The authors declare that they have no competing interests.

Funding: This work was supported financially by the National Natural Science Fundation of China (81803512), the Scientific Research and Cultivation Fundation for young teachers of pharmacy of Guangdong Pharmaceutical University, the Scientific Research Projects (Characteristic Innovation) of General Universities in Guangdong Province (2019KTSCX195) and the Initial Scientific Research Fundation of Doctor in Foshan University (CGG07246).

Authors' contributions: Haiyun Chen: Formal analysis, Data curation, Writing, Validation, Supervision, Conceptualization, Project administration, Funding acquisition. **Xiao Chang**: Investigation. **Jiemei Zhou**: Investigation. **Guiliang Zhang**: Investigation. **Jiehong Cheng**: Investigation. **Zaijun Zhang**: Investigation. **Zheng Liu**: Conceptualization, Project administration, Funding acquisition, Writing - review &editing. **Chuanyan Yan**: Supervision, Project administration, Conceptualization.

Acknowledgements: Not applicable.

References

1. Venegas C, Heneka MT: Inflammasome-mediated innate immunity in Alzheimer's disease. Faseb j. 2019; 33:13075-13084.

2. Loera-Valencia R, Cedazo-Minguez A, Kenigsberg PA, Page G, Duarte AI, Giusti P, Zusso M, Robert P, Frisoni GB, Cattaneo A, et al: Current and emerging avenues for Alzheimer's disease drug targets. J Intern Med. 2019; 286:398-437.

3. Long JM, Holtzman DM: Alzheimer Disease: An Update on Pathobiology and Treatment Strategies. Cell. 2019; 179:312-339.

4. Colonna M, Butovsky O: Microglia Function in the Central Nervous System During Health and Neurodegeneration. Annu Rev Immunol. 2017; 35:441-468.

5. Ozben T, Ozben S: Neuro-inflammation and anti-inflammatory treatment options for Alzheimer's disease. Clin Biochem. 2019; 72:87-89.

6. Monty L, Dafydd GL, Xunming J, Marcela PV, Daqing M: Neuroinflammation: The role and consequences. Neuroscience Research. 2014; 79:1-12.

7. Hammond TR, Marsh SE, Stevens B: Immune Signaling in Neurodegeneration. Immunity. 2019; 50:955-974.

8. Abner. EMWTLSEL, Mendenhall. GJPMD, Greenstein. HMBKBA, Wilcock. DM: Transition from an M1 to a mixed neuroinflammatory phenotype increases amyloid deposition in APP/PS1 transgenic mice. Journal of Neuroinflammation. 2014; 11:127.

9. Nicole M, Xu G, Kokiko-Cochran ON, Jiang S, Astrid C, Ransohoff RM, Lamb BT, Kiran B: Reactive microglia drive tau pathology and contribute to the spreading of pathological tau in the brain. Brain A Journal of Neurology. 2015; 138:1738-1755.

10. Dheen ST, Kaur C, Ling EA: Microglial activation and its implications in the brain diseases. Curr Med Chem. 2007; 14:1189-1197.

11. Garden GA, Möller T: Microglia biology in health and disease. Journal of neuroimmune pharmacology. 2006; 1:127-137.

12. Chen L, Jin Z, Xiaopeng S, Shan M, Linlin B, Song Z, Qian Y, Xuanxuan Z, Meng Z, Yanhua X: Neuroprotective Effects of Tetramethylpyrazine against Dopaminergic Neuron Injury in a Rat Model of Parkinson's Disease Induced by MPTP. International Journal of Biological Sciences. 2014; 10:350-357.

13. Zhao H, Xu M-L, Zhang Q, Guo Z-H, Peng Y, Qu Z-Y, Li Y-N: Tetramethylpyrazine Alleviated Cytokine Synthesis and Dopamine Deficit and Improved Motor Dysfunction in the Mice Model of Parkinson's Disease. Neurological Sciences 2014; 35:1963-1967.

14. Zhang G, Wu J, Huang C, Cheng J, Su Z, Zhu Z, Yang X, Guo B, Wu L, Zhang Z, et al: The Tetramethylpyrazine Analogue T-006 Alleviates Cognitive Deficits by Inhibition of Tau Expression and Phosphorylation in Transgenic Mice Modeling Alzheimer's Disease. Journal of Molecular Neuroscience. 2021; 71:1456-1466.

15. Zhong J, Qiu X, Yu Q, Chen HY, Yan CY: A novel polysaccharide from Acorus tatarinowii protects against LPS-induced neuroinflammation and neurotoxicity by inhibiting TLR4-mediated MyD88/NF-κB and PI3K/Akt signaling pathways. Int J Biol Macromol. 2020; 163:464-475.

16. Xia C, Iyc B, Tsc C, You H, Chan Y, Cfw A, Khk E, Wkk B: Pretreatment with interferon-γ protects microglia from oxidative stress via up-regulation of Mn-SOD - ScienceDirect. Free Radical Biology and Medicine. 2009; 46:1204-1210.

17. Zhou Y, Chen Y, Xu C, Zhang H, Lin C: TLR4 Targeting as a Promising Therapeutic Strategy for Alzheimer Disease Treatment. Frontiers in Neuroscience. 2020; 14:602508.

18. Xu D, Chen H, Mak S, Hu S, Tsim K, Hu Y, Sun Y, Zhang G, Wang Y, Zhang Z: Neuroprotection against glutamate-induced excitotoxicity and induction of neurite outgrowth by T-006, a novel multifunctional derivative of tetramethylpyrazine in neuronal cell models. Neurochemistry International. 2016; 99:194-205.

19. Heneka MT, Carson MJ, El Khoury J, Landreth GE, Brosseron F, Feinstein DL, Jacobs AH, Wyss-Coray T, Vitorica J, Ransohoff RM, et al: Neuroinflammation in Alzheimer's disease. Lancet Neurol. 2015; 14:388-405.

20. Wang XX, Wang CM, Wang JM, Zhao SQ, Zhang K: Pseudoginsenoside-F11 (PF11) exerts anti-neuroinflammatory effects on LPS-activated microglial cells by inhibiting TLR4-mediated TAK1/IKK/NF-κB, MAPK and Akt signaling pathways. Neuropharmacology. 2014; 79:642-656.

21. Muhammad T, Ikram M, Ullah R, Rehman S, Kim M: Hesperetin, a Citrus Flavonoid, Attenuates LPS-Induced Neuroinflammation, Apoptosis and Memory Impairments by Modulating TLR4/NF-κB Signaling. Nutrients. 2019; 11:648.

22. Yang YL, Liu M, Cheng X, Li WH, Zhang SS, Wang YH, Du GH: Myricitrin blocks activation of NF-κB and MAPK signaling pathways to protect nigrostriatum neuron in LPS-stimulated mice. J Neuroimmunol. 2019; 337:577049.

23. Zhao M, Zhou A, Xu L, Zhang X: The role of TLR4-mediated PTEN/PI3K/AKT/NF-κB signaling pathway in neuroinflammation in hippocampal neurons. Neuroscience. 2014; 269:93-101.

24. M Z, V L, D F, A P, R L, S S, AC F, P G, S M: Ciprofloxacin and levofloxacin attenuate microglia inflammatory response via TLR4/NF-kB pathway. J Neuroinflamm. 2019; 16:148.

25. Li CW, Chen TK, Zhou HF, Yu F, Hoi MPM, Dan M, Chao Z, Ying Z, Lee SMY: BHDPC Is a Novel Neuroprotectant That Provides Anti-neuroinflammatory and Neuroprotective Effects by Inactivating NF-κB and Activating PKA/CREB. Front Pharmacol. 2018; 9:1-15.

26. Lu YC, Yeh WC, Ohashi PS: LPS/TLR4 signal transduction pathway. Cytokine. 2008; 42:145-151.

27. West AP: Mitochondrial dysfunction as a trigger of innate immune responses and inflammation. Toxicology. 2017; 391:54-63.

28. Whitney NP, Eidem TM, Peng H, Huang Y, Zheng JC: Inflammation mediates varying effects in neurogenesis: relevance to the pathogenesis of brain injury and neurodegenerative disorders. J Neurochem. 2009; 108:1343-1359.

29. Mawuenyega KG, Sigurdson W, Ovod V, Munsell L, Kasten T, Morris JC, Yarasheski KE, Bateman RJ: Decreased Clearance of CNS β-Amyloid in Alzheimer's Disease. Science. 2010; 330:1774.

30. Zhang YW, Thompson R, Zhang H, Xu H: APP processing in Alzheimer's disease. Mol Brain. 2011; 4:3.

31. Walker KA, Ficek BN, Westbrook R: Understanding the Role of Systemic Inflammation in Alzheimer's Disease. ACS Chemical Neuroscience. 2019; 10:3340-3342.

32. Fu A, Hung KW, Yuen M, Zhou X, Mak D, Chan I, Cheung TH, Zhang B, Fu WY, Liew FY: IL-33 ameliorates Alzheimer's disease-like pathology and cognitive decline. Proc Natl Acad Sci U S A. 2016; 113:201604032.

33. Jin X, Liu MY, Zhang DF, Zhong X, Du K, Qian P, Yao WF, Gao H, Wei MJ: Baicalin mitigates cognitive impairment and protects neurons from microglia-mediated neuroinflammation via suppressing NLRP3 inflammasomes and TLR4/NF-κB signaling pathway. CNS Neuroscience & Therapeutics. 2019; 25:575-590.

34. Peri F, Calabrese V: Toll-like receptor 4 (TLR4) modulation by synthetic and natural compounds: an update. J Med Chem. 2014; 57:3612-3622.

35. Fu-Yi, Liu, Jing, Cai, Chun, Wang, Wu, Ruan, Guo-Ping, Guan: Fluoxetine attenuates neuroinflammation in early brain injury after subarachnoid hemorrhage: a possible role for the regulation of TLR4/MyD88/NF-κB signaling pathway. Journal of Neuroinflammation. 2018; 15:347.

36. Christophe M, Nicolas S: Mitochondria: a target for neuroprotective interventions in cerebral ischemia-reperfusion. Curr Pharm Des. 2006; 12:739-757.

Figures

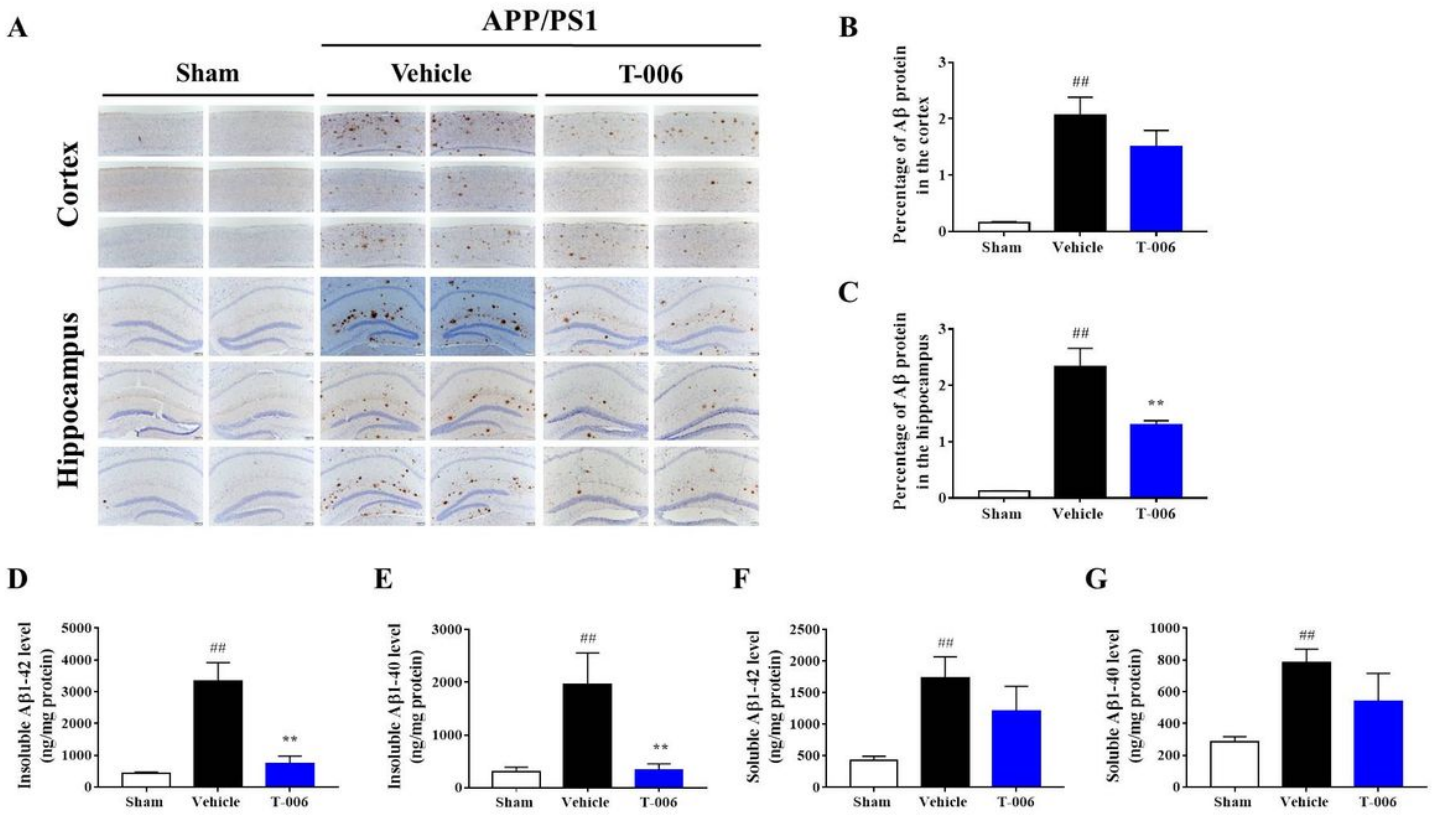

Figure 1

T-006 alleviated the Aβ accumulation in the hippocampus of the APP/PS1 mice. (A) Immunohistochemical analysis of brains after administration of T-006 for 8 months. The levels of Aβ in the brains were stained by anti-Aβ anti-body. (B-C) The quantitative statistics of Aβ expression levels in cortex and hippocampus. (D-G) The amount of soluble and insoluble Aβ fractions extracted from hippocampus. Data are expressed as mean ± SEM with n = 3 mice per group. ##p<0.01 versus sham group (WT mice); **p<0.01 versus vehicle group (APP/PS1 mice).

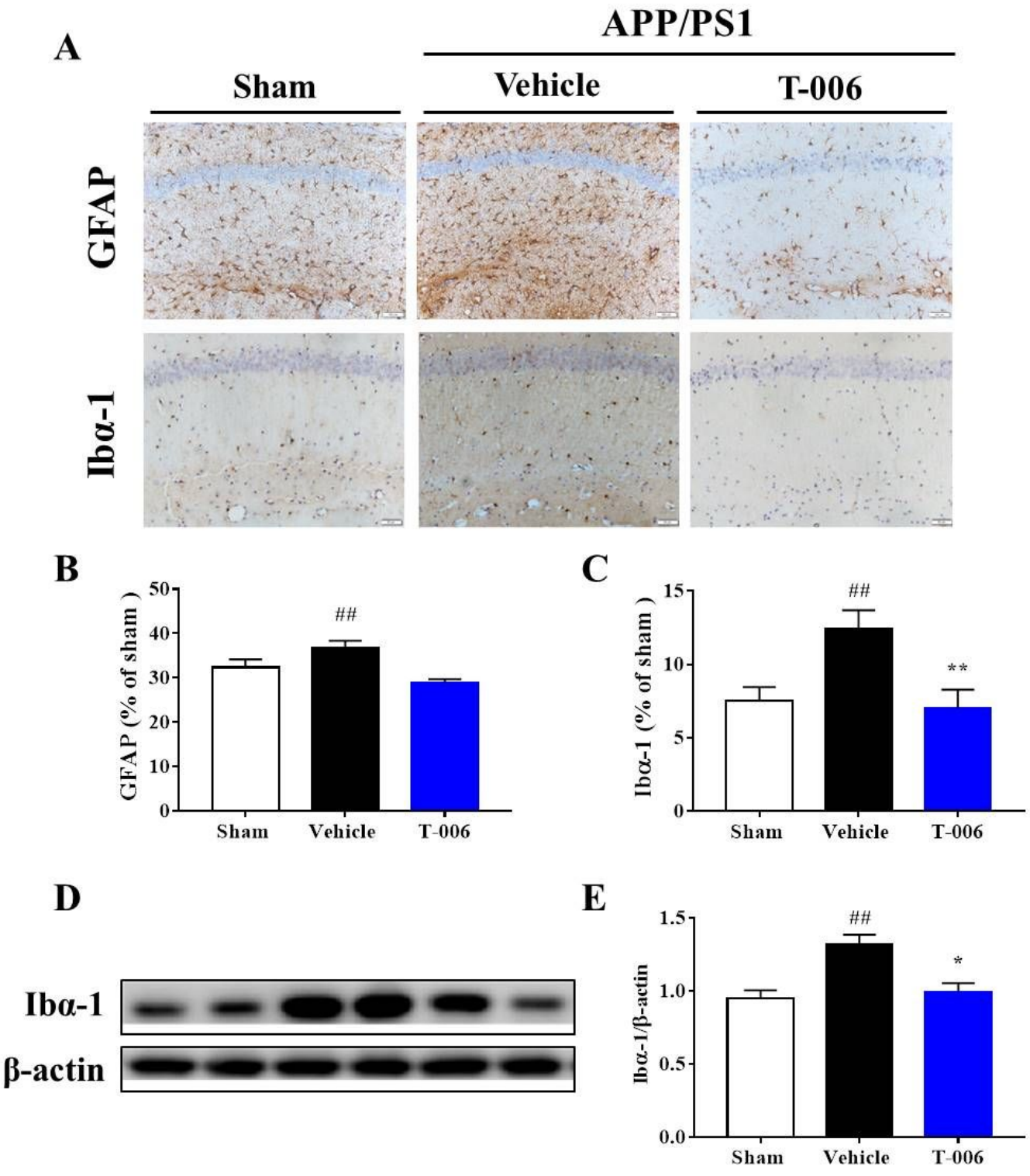

Figure 2

T-006 suppressed neuroinflammation in the APP/PS1 mice. (A) Immunohistochemical analysis of brains after administration for 8 months. The levels of astrocytic and microglial activation in the hippocampus were stained by GFAP and Ibα-1 anti-bodies, respectively. (B-C) The quantitative statistic of GFAP and Ibα-1 proteins expression levels in hippocampus. (D-E) Western blot results of Ibα-1. Data are expressed as mean ± SEM with n = 3 mice per group. ##p<0.01 versus sham group (WT mice); **p<0.01 versus vehicle group (APP/PS1 mice).

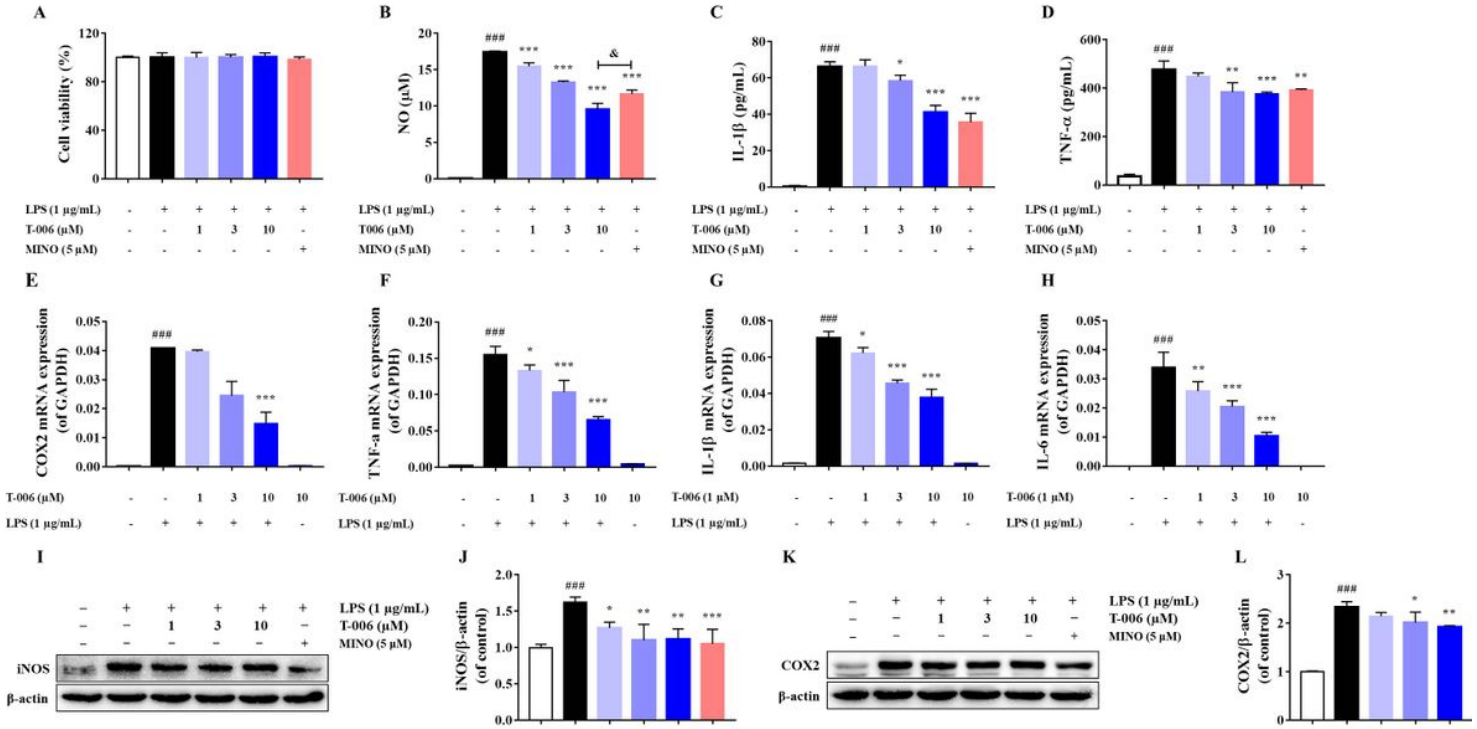

Figure 3

T-006 diminished LPS-stimulated pro-inflammatory responses in BV2 microglial cells. (A) MTT assay. (B) NO production. (C-D) The levels of IL-1β and TNF-α, respectively. (E-H) the changes of the mRNA levels of COX-2, TNF-α, IL-1β and IL-6 normalized to that of GAPDH. (I-J) Western blot results of iNOS. (K-L) Western blot results of COX2. Data are expressed as mean ± SEM with three independent experiments. MINO was used as a positive control drug. ###p < 0.001 versus control group; *p < 0.05, **p < 0.01, ***p < 0.001 versus LPS group; and &p < 0.05 versus MINO group.

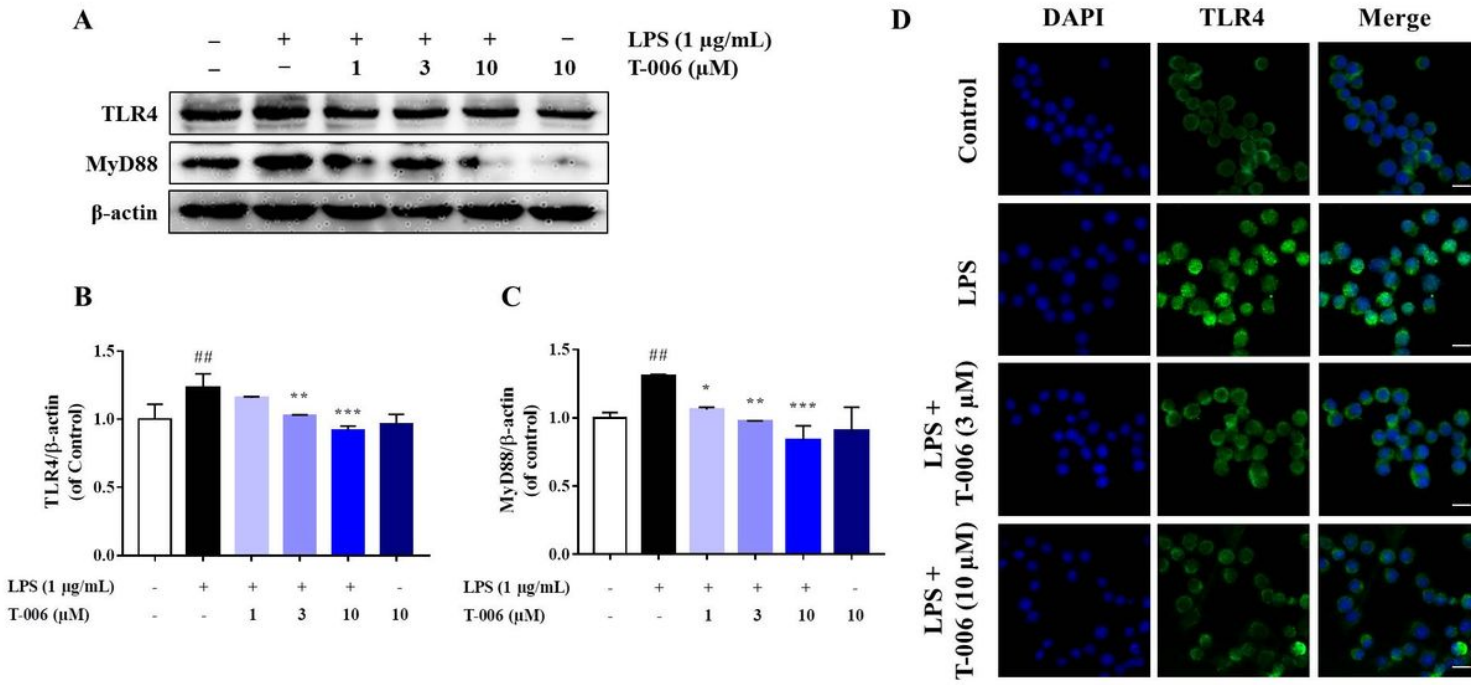

Figure 4

Suppressive effects of T-006 on expression of TLR4 and MyD88 in LPS-induced BV2 microglial cells. (A) Western blots signal bands of TLR4 and MyD88. (B, C) Quantitative analysis of (A). (D) Immunofluorescence images of cells co-stained with antibodies against TLR4 (green). DAPI (blue) indicates nucleus. Scale bar = 20 μm. Data are expressed as mean ± SEM with three independent experiments. Control denotes normal-medium cultured cells. ##p < 0.01 versus control group; *p < 0.05, **p < 0.01, ***p < 0.001 versus LPS group.

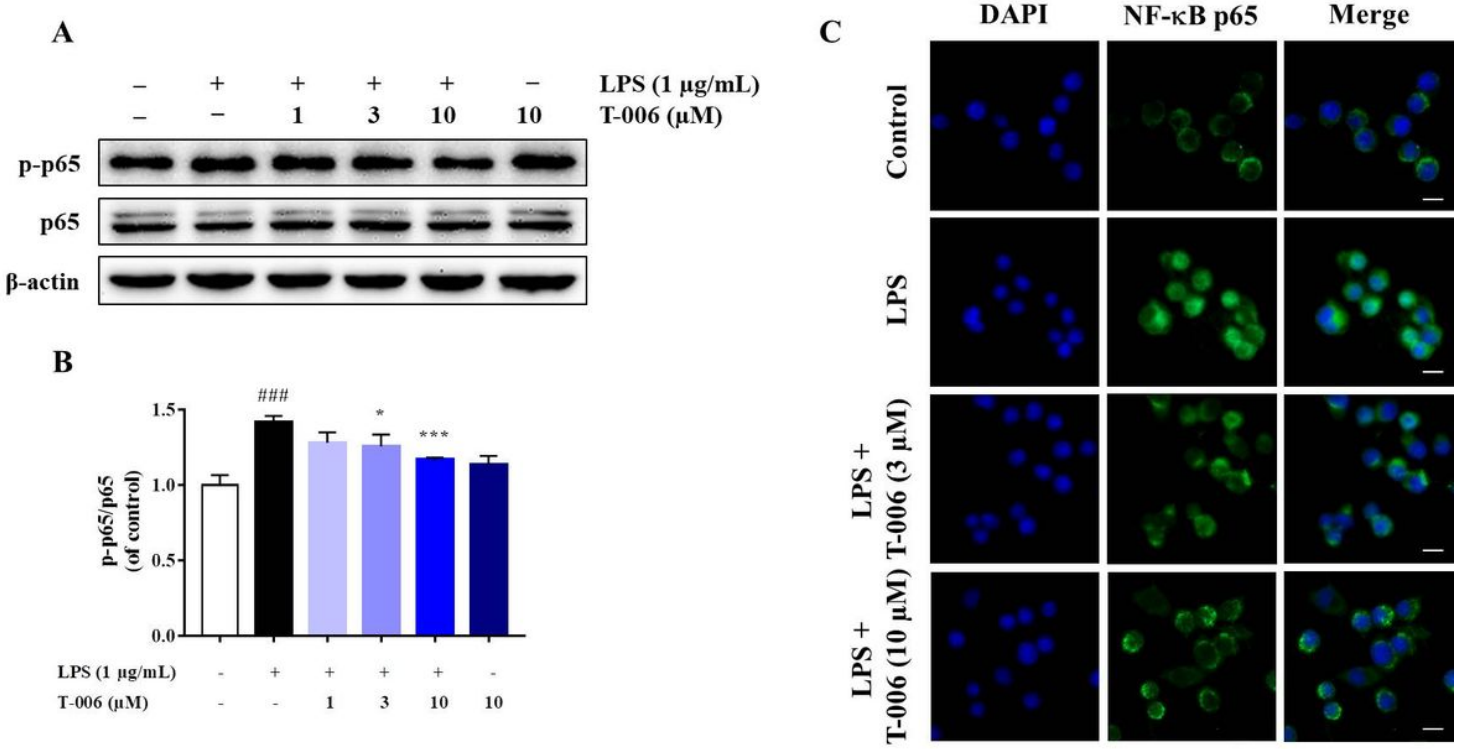

Figure 5

Suppressive effects of T-006 on activation of NF-κB in LPS-induced BV2 microglial cells. (A) Western blots signal bands of phosphorylated-NF-κB p65 and NF-κB p65. (B) Quantitative analysis of (A). (C) Immunofluorescence images of cells co-stained with antibodies against NF-κB p65 (green). DAPI (blue) indicates nucleus. Scale bar = 20 μm. Data are expressed as mean ± SEM with three independent experiments. ###p < 0.001 versus control group; *p < 0.05, ***p < 0.001 versus LPS group.

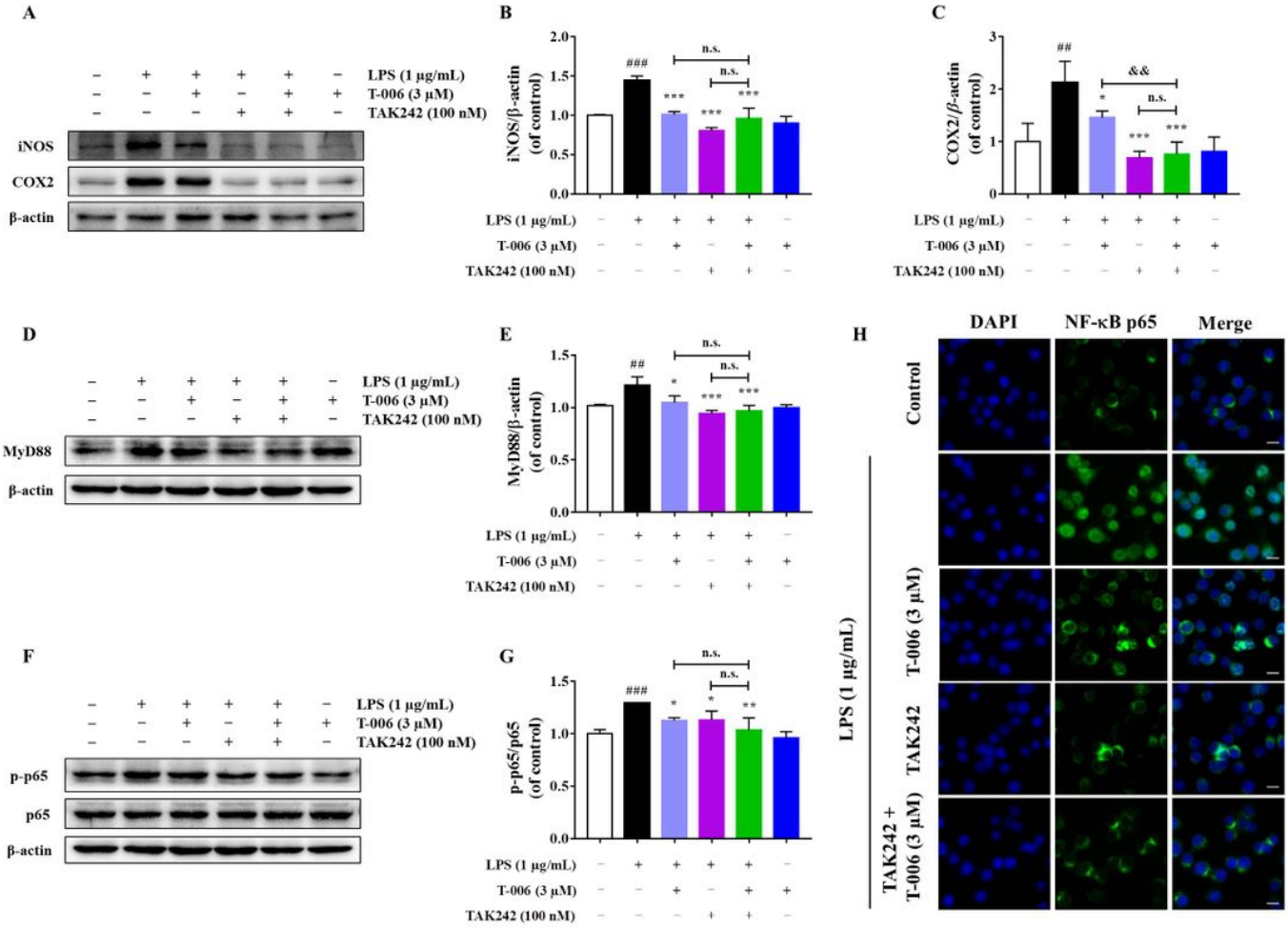

Figure 6

T-006 diminished LPS-induced proinflammatory cytokines levels through suppression of TLR4-mediated MyD88/NF-κB pathway. (A) Western blot signal bands of iNOS and COX-2. (B, C) Quantitative analysis of (A). (D) Western blot signal band of MyD88. (E) Quantitative analysis of (D). (F) Western blot signal bands of phosphorylated NF-κB p65. (G) Quantitative analysis of (F). (H) Immunofluorescence images of cells co-stained with antibodies against NF-κB p65 (green). DAPI (blue) indicates nucleus. Scale bar = 20 μm. Data are expressed as mean ± SEM with three independent experiments. ##P < 0.01, ###p < 0.001 versus control group; *p < 0.05, **p < 0.01, ***p < 0.001 versus LPS group; &&p < 0.01 versus T-006 or TAK242 group.

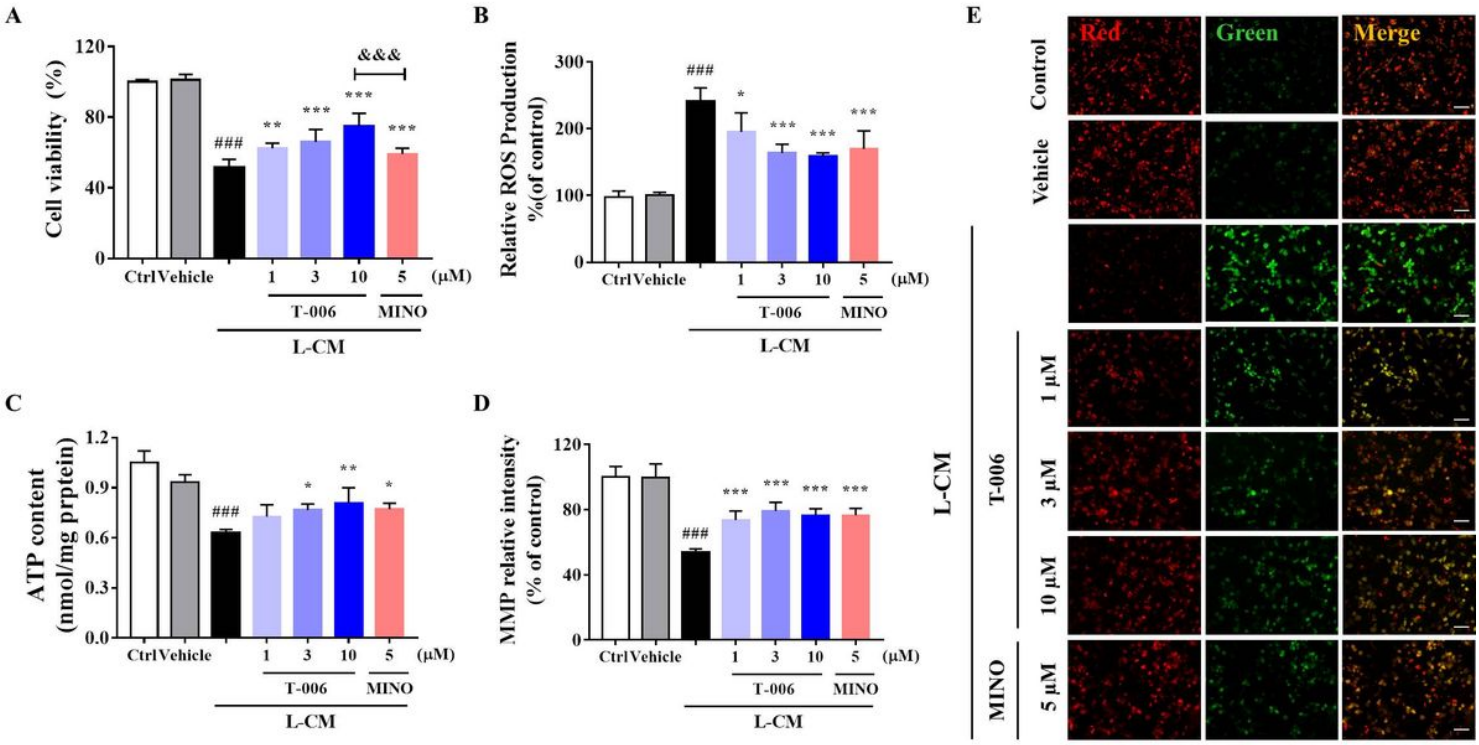

Figure 7

T-006 prevented LPS-activated BV2 microglia-mediated neurotoxicity in PC12 cells. (A) Cell viability was measured using the MTT assay. (B) ROS production assessed by DCF fluorescence intensity. (D) MMP tested by JC-1 kit. (E) Immunofluorescence images. Red indicates aggregates. Green indicates monomer. Scale bar = 20 μm. L-CM denotes the supernatants from the BV2 microglial cells treated with 1 μg/mL LPS for 24 h. Data are as mean ± SEM with three independent experiments. ###p < 0.001 versus control group; and *p < 0.05, **p < 0.01, ***p < 0.001 versus L-CM group; &&&p < 0.001 versus MINO group.